2011 American Control Conference
on O'Farrell Street, San Francisco, CA, USA
June 29 - July 01, 2011

Optimal Energy Management for a Flywheel-Based Hybrid Vehicle

Koos van Berkel, Theo Hofman, Bas Vroemen, Maarten Steinbuch

Abstract— **This paper presents the modeling and design of an optimal Energy Management Strategy (EMS) for a flywheel-based hybrid vehicle, that does not use any electrical motor/generator, or a battery, for its hybrid functionalities. The hybrid drive train consists of only low-cost components, such as a flywheel module and a continuously variable transmission. This hybrid drive train is characterized by a relatively small energy capacity (flywheel) and discrete shifts between operation modes, due to the use of clutches. The main design criterion of the optimized EMS is the minimization of the overall fuel consumption, over a pre-defined driving cycle. In addition, comfort criteria are formulated as constraints, e.g., to avoid high-frequent shifting between driving modes. The criteria are used to find the optimal sequence of driving modes and the generated engine torque. Simulations show a fuel saving potential of 20% to 39%, dependent on the chosen driving cycle.**

Index Terms— **Optimal control, Modeling and Simulation, Automotive**

I. INTRODUCTION

Hybrid vehicles, i.e., vehicles that use a secondary power source, are a promising solution to the problem of reducing the fuel consumption and carbon dioxide emission of passenger vehicles. For the emerging vehicle market in, e.g., China, hybridization of vehicles is of great interest due to the increasing oil price and stricter environmental legislation. However, the additional cost of most hybrid transmissions, as compared to their conventional counterparts, is relatively high due to costly electrical components, such as large battery packs, high-power electronic power converters, and additional motor(s) and/or generator(s). Such high additional cost may not be acceptable in this cost-sensitive market.

In this paper we present a low-cost *mecHybrid*-drive train design, using a steel-flywheel module and a push-belt Continuously Variable Transmission (CVT), for energy storage and power transmission, respectively. The modular design of the hybrid drive train is schematically depicted in Fig. 1. This concept uses the CVT to "charge" the flywheel with the vehicle's kinetic energy to brake the vehicle, and to reuse this energy to propel the vehicle [1]. This hybrid drive train has a low-cost potential due to the following design choices [2]: (1) the hybrid module contains only low-cost mechanical components, such as a steel flywheel, gears and compact clutches; (2) the added production complexity is limited, due to its modular design; and (3) current CVTs have become a mature, low-cost and fuel-efficient technology [3]. The main fuel saving benefit can be attributed to the added hybrid functionalities: recuperation of brake energy, driving purely on the flywheel, and engine shut-off during standstill, which are considered as very effective measures in reducing the fuel consumption [4]. Other fuel saving techniques, e.g. by improving the transmission efficiency of the CVT with slip control [5] or extremum seeking control [6], are not discussed here. In this paper we will not consider the design issues related to sizing and choice of components, but we will address energy management strategies for such hybrids.

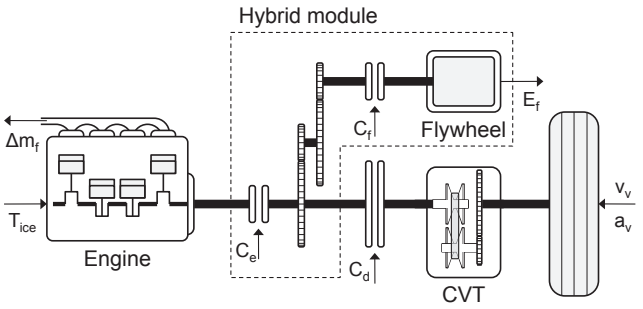

Fig. 1. Hybrid drive train topology and signal flow, including the flywheel module, clutches and Continuously Variable Transmission (CVT).

A. Energy Management Strategy

To make full use of the hybrid functionalities, an Energy Management Strategy (EMS) is required, that manages the power flows at system level, by creating set-points for the low-level sub-system controllers, which control the dynamics in the hybrid drive train. One of the main questions regarding this controller is [7]: *how can the secondary mover, i.e., flywheel system, be utilized to minimize the fuel consumption, without compromising comfort issues such as engine noise?* In literature, various EMS design approaches are described for hybrid vehicles, see, e.g., [8] for an overview. EMS designs may be classified into heuristic, optimal and sub-optimal controllers [4]. Strategies that are based on heuristics can be very suitable for online-implementation, by using a rule-based [9], or fuzzy logic strategy [10]. Although these strategies offer a significant improvement in fuel economy with a relatively simple control design, it is not clear whether the result is close to the optimal solution in all situations. Optimal strategies use global optimization techniques such

This work is a part of the mecHybrid project which is a common project of DTI, Punch Powertrain, CCM, Bosch, SKF, and TU/e. The project is partly funded by the Dutch Ministry of Economic Affairs, Provincie Noord-Brabant and SRE.

K. van Berkel, T. Hofman, and M. Steinbuch are with the Department of Mechanical Engineering, Eindhoven University of Technology, P.O. box 513, 5600 MB Eindhoven, The Netherlands, Phone: +31 40 247 2811, Fax: +31 40 246 1418, k.v.berkel@tue.nl, t.hofman@tue.nl, m.steinbuch@tue.nl.

B. Vroemen is with Drivetrain Innovations, Croy 46, 5653 LD Eindhoven, The Netherlands, vroemen@dtinnovations.nl.

as Linear Programming (LP), (Sequential) Quadratic Programming ((S)QP) and Dynamic Programming (DP) [11]. With the LP and (S)QP optimization techniques, the in general non-linear drive train model is linearized to fit to the optimization framework, such that the optimization problem becomes convex. With DP, the global solution can be found for non-convex optimization problems [12]. In general, these optimal techniques do not offer a online-implementable (or causal) solution, because they assume that the future driving profile is exactly known. Nevertheless, their result can be used as a benchmark for the performance of other strategies, or for the design of sub-optimal causal strategies. Sub-optimal strategies combine the benefits of both optimal and causal controllers, which result in a causal, yet close-to-optimal EMS, such as described in [4].

B. Main Contribution and Outline

EMS design approaches for hybrid electric vehicles are well covered in literature, e.g., as described in [13]. Mechanical-hybrid vehicles, however, may have different characteristics:

- a relatively small energy storage capacity;
- discrete shifts between driving modes; and
- relatively many kinematic constraints in the drive train.

Kinematic constraints in the drive train may cause undesired engine noise, when the engine noise does not match the driver's expectation, e.g., a steadily decreasing engine noise frequency during full power demand. For mechanical-hybrid vehicles, few optimal EMS design approaches are found. In [10], [14], heuristic strategies that consider discrete driving mode shifts and a small energy storage capacity are presented. Optimal strategies are found in [15], [16], but do not consider discrete shifts between driving modes.

This paper presents an optimal EMS for a flywheel-based mechanical-hybrid vehicle, including the characteristics as described above. The main design criterion of the optimal EMS, is the minimization of the overall fuel consumption, over a pre-defined driving cycle. In addition, constraints are defined satisfying the system's kinematics and dynamics for each driving mode, but also for shifts in between. Furthermore, *comfort constraints* are defined to avoid uncomfortable situations. DP is applied to find the optimal sequence of driving modes and the generated engine torque.

The outline is given as follows: Section II describes the modeling of the base components. Section III describes the hybrid drive train model for different driving modes, and for shifts in between. Section IV defines and solves the optimization problem using DP. Furthermore, problem reductions are proposed. Section V presents the simulation results for five typical driving cycles. Finally, Section VI presents conclusions and future work.

II. COMPONENT MODELS

The main components of the hybrid drive train are the Internal Combustion Engine (ICE), flywheel system (FW), clutches, CVT, and vehicle. Table I summarizes some characteristics. This section describes the modeling of these components. Some (efficiency) models are, because of their non-linear behavior, described by *look-up tables*, based on static experiments, under warm operating conditions. For such models, intermediate points are calculated by linear interpolation. Dynamic effects, such as drive train oscillations, are not considered. Fig. 2 shows the resulting dynamic model of the hybrid drive train.

TABLE I
BASE COMPONENT CHARACTERISTICS

Engine[1]	4-cylinder 1.5-l gasoline int. comb. engine, max. power 76 kW (at 6000 rpm), max. torque 140 Nm (at 4000 rpm), peak efficiency 230 g/kWh.
Flywheel[1]	Vacuum-placed 150-kJ steel flywheel, max. power 35 kW, max. speed 30.000 rpm, inertia 0.03 kgm^2, gear ratio 1:12, total module mass 27 kg, drag torque 0.07-0.11 Nm.
Transmission[1]	Push-belt driven Continuously Variable Transmission, max. input torque 140 Nm, ratio range 6.0, final drive ratio 1:5.41, integrated pump, max. efficiency 91%.
Vehicle[2] + 2 passengers	Smart ForFour (2005), mass 970+150 kg, inertia of all wheels 1.2 kgm^2, aerodynamic drag coefficient 0.31, frontal area 1.86 m^2, rolling resistance 143 N.

[1]Data based on experimental results. [2]Data based on estimated parameters.

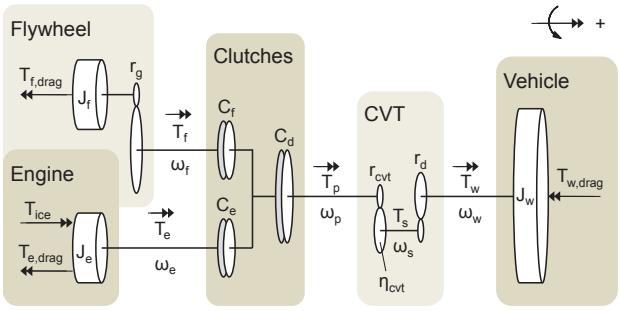

Fig. 2. Dynamic model of the hybrid drive train (compliances are omitted).

A. Internal Combustion Engine

The ICE model is based on its inertia J_e, on which three torques are acting: the generated torque T_{ice}, drag torque $T_{e,drag}$, and external torque T_e. Here, T_e depends on the selected driving mode, as described in Section III-A. The dynamics and constraints in discrete time format, using a simple forward Euler scheme, are given by

$$\omega_{e,k+1} = \omega_{e,k} + \frac{1}{J_e}(T_{ice,k} - T_{e,drag,k} - T_{e,k}), \quad (1)$$

$$0 \leq T_{ice,k} \leq T_{e,WOT}(\omega_{e,k}), \quad (2)$$

$$\omega_{e,min} \leq \omega_{e,k} \leq \omega_{e,max}. \quad (3)$$

with a fixed time step $\Delta T = 1$ s. The discrete time sample is indicated by subscript "k". Here, ω_e is the rotational speed of the ICE and $T_{e,WOT}$ the generated *Wide-Open-Throttle* torque, described by a look-up table. The ICE's drag torque, $T_{e,drag,k} = T_{e,drag}(\omega_{e,k})$, is modeled as a second

order polynomial for positive speeds, using nonnegative coefficients based on experimental results, and equals zero at zero speed. The injected fuel mass rate (g/s) is described by a look-up table: $\Delta m_{f,k} = \Delta m_f(\omega_{e,k}, T_{ice,k})$.

B. Flywheel

The FW model is based on its inertia J_f, on which two torques are acting: the drag torque $T_{f,drag}$ and external torque T_f (depends on the driving mode cf. with Section III-A). The dynamics and constraints are given by

$$\omega_{f,k+1} = \omega_{f,k} + \frac{r_g^2}{J_f}\left(\frac{-T_{f,k}}{\eta_{g,k}} - \frac{T_{f,drag,k}}{r_g}\right), \quad (4)$$

$$\omega_{f,min} \leq \omega_{f,k} \leq \omega_{f,max}. \quad (5)$$

Here, ω_f is the rotational speed of the output shaft of the FW system. The drag torque describes the system's bearing-, seal-, and air drag losses acting on the rotor, and is modeled as a second order polynomial for positive speeds ($T_{f,drag,k} = T_{f,drag}(\omega_{f,k})$), using nonnegative coefficients based on experimental results, as shown in [1]. The gear gives a constant gear ratio r_g between ω_f and the rotor. The gear's transmission efficiency is described, for both positive and negative torques, by a look-up table, i.e., $\eta_{g,k} = \eta_g(T_{f,k})$. There are no explicit constraints on T_f, but the torque on the CVT's input shaft is constrained, as will be described below. The FW's energy content E_f (J) equals

$$E_{f,k} = \frac{J_f}{2r_g^2}\omega_{f,k}^2. \quad (6)$$

C. Clutches

The hybrid powertrain contains three actively controlled clutches: the *engine clutch* (subscript "e"), *flywheel clutch* (subscript "f"), and *drive clutch* (subscript "d"). The engine- and flywheel clutch are used to select the mover (i.e., ICE, or FW), as will be described in Section III-A. A discrete clutch state is used: $C_x = 0$ when disengaged and $C_x = 1$ when engaged, for $x \in \{e, f\}$. It is assumed that the clutches (dis)engage within one time step; the corresponding additional power losses are discussed in Section III-B. The drive clutch will be used to launch the vehicle from standstill. During a launch, the CVT's speed ratio is kept at $r_{ctv,min}$, while the clutch slips with slip speed ω_c. The transmitted torque (T_p) is assumed to be accurately controlled, such that the dissipated power equals

$$P_{clutch} = T_p|\Delta\omega_c|. \quad (7)$$

D. CVT

The CVT provides a variable speed ratio $r_{cvt,k} = \omega_{s,k}/\omega_{p,k}$ between the primary- (subscript "p") and secondary pulley shaft (subscript "s"). The final drive gives a constant speed ratio $r_d = \omega_w/\omega_s$ between the secondary pulley shaft and the wheel shaft (subscript "w"). Constraints apply to r_{cvt}, its change $\Delta r_{cvt,k} = r_{cvt,k+1} - r_{cvt,k}$, and primary torque T_p:

$$r_{cvt,min} \leq r_{cvt,k} \leq r_{cvt,max}, \quad (8)$$

$$-c\ r_{cvt,k} \leq \Delta r_{cvt,k} \leq c\ r_{cvt,k}, \quad (9)$$

$$T_{p,min} \leq T_{p,k} \leq T_{p,max}. \quad (10)$$

Here, the shift-speed constraint is modeled as in [17], with shift-speed constant $c = 1$. The transmission efficiency of the CVT system is described, for both positive and negative torques, with a look-up table: $\eta_{cvt,k} = \eta_{cvt}(\omega_{w,k}, T_{w,k}, r_{cvt,k})$. The transmission efficiency includes losses by the pump and final drive, using a conventional control strategy, as described in [18].

E. Vehicle

The vehicle is modeled by the inertia of the wheels J_w, including the total vehicle mass and two passengers (of 75 kg), on which three torques are acting: drag torque $T_{w,drag}$, the torque at the wheel side of the CVT T_w, and brake torque T_b. For given vehicle velocity v_v and acceleration a_v, and neglecting any wheel slip, the required T_w equals

$$T_{w,k} = T_{w,drag,k} + \frac{J_w}{r_w}a_{v,k} + T_{b,k}. \quad (11)$$

Here, $T_{w,drag,k} = T_{w,drag,}(v_{v,k})$ is modeled as a second order polynomial for positive velocity, using nonnegative coefficients based on estimated parameters of the vehicle, and equals zero at standstill. The brake is used when brake energy recuperation is constrained, e.g., by the selected driving mode, or (10). The effective wheel radius gives a constant speed ratio: $r_w = v_v/\omega_w$.

III. HYBRID DRIVE TRAIN MODEL

For a pre-defined driving cycle, the hybrid drive train can be controlled with two control inputs (i.e., $u = [u_1, u_2]^T$): the next driving mode of the hybrid drive train, as will be explained below, and the generated engine torque, such that $u_k := [\phi_{k+1}, T_{ice,k}]^T$. Instead of $T_{ice,k}$, one may also choose r_{cvt} to control operation point of the ICE. Here, T_{ice} is selected, which seems logical from a physical point of view; this degree of freedom only exists when the ICE is engaged. Furthermore, three states can be defined (i.e., $x_k = [x_1, x_2, x_3]^T$): the speeds of the ICE and FW, to describe their dynamics, and current driving mode to detect driving mode shifts, such that $x_k := [\omega_{e,k}, \omega_{f,k}, \phi_k]^T$. The pre-defined driving cycle is introduced as a disturbance $w_k := (v_{v,k}, a_{v,k})^T$. This section describes the hybrid drive train dynamics for each driving mode, as well as for the shifts in between.

A. Driving Modes

Three quasi-static driving modes are identified, in which the engine- and flywheel clutch are not slipping (i.e., they can be either disengaged or engaged). Driving mode $\phi \in \{1, 2, 3\}$ is defined by the states of these clutches (C_e, C_f) and prescribes which mover is used to propel the vehicle with.

$$\phi(C_e, C_f) := \begin{cases} 1, & \texttt{if} \quad C_e = 0, \quad C_f = 1, \\ 2, & \texttt{if} \quad C_e = 1, \quad C_f = 1, \\ 3, & \texttt{if} \quad C_e = 1, \quad C_f = 0. \end{cases} \quad (12)$$

1) FW Driving ($\phi = 1$): the CVT is used to either propel, or brake the vehicle with the FW, while the ICE is disengaged and is shut-off.

2) FW Charging ($\phi = 2$): the ICE propels the vehicle, while simultaneously, the FW is "charged" ($T_f < 0$), or "discharged" ($T_f > 0$) to assist the ICE. The (dis-)charging torque T_f is controlled by T_{ice}. Although beneficial for acceleration performance, ICE assist is not supported as, due to the mechanical connection between the FW and ICE, the ICE decelerates with the FW. A decelerating ICE implies (i) a decreasing ICE torque, such that performance reduces until the ICE runs at "idle" speed; and (ii) a decreasing ICE noise frequency, while the driver expects an increasing noise frequency with high power demand. To avoid these situation, the following constraint is introduced:

$$u_{2,k} \in \{T_{ice,k} \mid T_{f,k} < 0, T_{w,k} \geq 0\}. \tag{13}$$

3) ICE Driving ($\phi = 3$): The ICE propels the vehicle, whereas the disc brakes brake the vehicle. The operation point of the ICE is controlled by T_{ice}.

For a given driving cycle, the wheel torque $T_{w,k}$ may be calculated with (11), such that $T_{p,k}$ equals

$$T_{p,k} = \eta_{cvt,k}^{-1}(\omega_{w,k}, T_{w,k}, r_{cvt,k}) r_{cvt,k} r_d T_{w,k}. \tag{14}$$

The required T_p is supplied by the external torque(s) of the engaged mover(s). For each driving mode, the required external torque of the mover(s) is summarized, as well as speed ratio r_{cvt}, in Table II. Note that, with Standstill and FW Driving, u_2 is undetermined, since the ICE is shut-off.

TABLE II
DRIVE TRAIN OPERATION DURING VARIOUS DRIVING MODES

ϕ	description	u_2	T_e^*	T_f^*	r_{cvt}^*
1	FW Driving	n/a	0	T_p	ω_s/ω_f
2	FW Charging	T_{ice}	$T_p - T_f$	$T_p - T_e$	ω_s/ω_f
3	ICE Driving	T_{ice}	T_p	0	ω_s/ω_e

*Constraints apply, see, (2), (3), (5), (8), (9), (10), (13), (16), (17).

B. Driving Mode Shifts

There are 6 different shifts possible between the 3 driving modes. These shifts may require additional actions by the drive train, or are constrained under certain conditions, as summarized in Table III. Notice that each shift takes one time step (or, 1 s), and, torque is transmitted through the drive train, while shifting from one mode to another.

1) ICE start: In this study, we assume that the FW always contains sufficient energy to crank the ICE. The additional torque $T_{f,start}$ to crank the ICE from $\omega_{e,k} = 0$ rad/s to $\omega_{e,k+1} = \omega_{f,k}$, is provided by the FW through the slipping engine clutch, and is modeled as:

$$T_{f,start,k} = J_e \frac{\omega_{e,k+1} - \omega_{e,k}}{\Delta T} + T_{e,drag}(\omega_{e,k+1}). \tag{15}$$

TABLE III
SHIFTS BETWEEN DRIVING MODES

ϕ_k	ϕ_{k+1}	actions / constraints
1	2	ICE Start, High-frequent Shifting
1	3	ICE Start, Disengage Mover
2	1	Disengage Mover
2	3	Disengage Mover
3	1	Synchronize, Disengage Mover
3	2	Synchronize

2) Disengage Mover: A mover is disengaged; no power is dissipated. Notice that, when the FW is disengaged, the ICE's speed might change, such that additional torque is required to accelerate or decelerate the ICE's inertia. The corresponding change in engine noise is expected to be acceptable, as in practice, this shift takes place when the vehicle's acceleration changes.

Next, two comfort-related constraints are defined.

3) Synchronize: When shifting from ICE Driving to FW Charging, or to FW Driving, the CVT is used to synchronize ω_e with ω_f, in order to synchronize the flywheel clutch, such that the movers can switch smoothly. Meanwhile, for $T_w \geq 0$, the ICE propels the vehicle. This synchronization may take a relatively long time for two reasons: (i) the shift speed of the CVT is relatively slow, as constrained by (9); and (ii) the synchronization has to be very accurate to avoid a torque peak, when quickly engaging the flywheel clutch (which is not designed to dissipate much energy), caused by the relatively large inertia of the FW. On the other hand, from a driver's comfort point of view, the powertrain has to be able to respond within an acceptable time frame, e.g., within 1 s. To avoid these issues, this mode shift is not supported, and hence constrained:

$$u_1 \in \{\phi \mid \phi_{k+1} = 3,\ \phi_k = 3, T_{f,k} \geq 0\}. \tag{16}$$

This mode shift is not constrained during braking ($T_w < 0$), to enable brake energy recuperation of ICE Driving. This shift also differs: during the shift, the disc brakes can decelerate the vehicle, such that the drive train is unloaded; the drive clutch is disengaged, such that the flywheel clutch can be engaged to synchronize the intermediate shaft with the FW; the unloaded CVT can shift quickly to the desired speed ratio, while the drive clutch can be used for a smooth synchronization.

4) High-frequent Shifting: Alternate shifting between FW Driving and FW Charging might be a fuel-efficient way to propel the vehicle at constant velocity. Especially at high constant velocities, when the shift-frequency increases, this shifting is expected to be uncomfortable for the driver, due to the alternating ICE noise. This comfort constraint is described using nonnegative coefficients a_c (m/s^2) and v_c (m/s), which define a "high, constant" velocity:

$$u_1 \in \{\phi \mid \phi_{k+1} = 2,\ \phi_k = 1, |a_{v,k}| < a_c, v_{v,k} > v_c\}. \tag{17}$$

IV. OPTIMIZATION

The control objective is to minimize the overall fuel consumption, over a pre-defined driving cycle of length N:

$$\min_{u_k} J = \sum_{k=1}^{N} \Delta m_f(x_k, u_k, w_k)\Delta T. \tag{18}$$

while respecting (1)-(12), (14), and (15) to describe the system's kinematics, dynamics, and constraints, and (13), (16), and (17) to avoid uncomfortable driving conditions. An end-value constraint for the FW's energy content is introduced to assure a zero net-energy balance of the FW, over the total driving cycle:

$$E_f(N) = E_f(1). \tag{19}$$

The signal flow of this optimization problem is schematically depicted in Fig. 1. Five driving cycles are considered: the Japan 10-15 mode (JP1015), Japan Cycle 08 (JC08), New European Driving Cycle (NEDC), Federal Test Procedure 75 (FTP75) and our own driving cycle (Hurk), see Fig. 3. The four standard cycles are widely used for certified fuel consumption measurements. The Hurk driving cycle is added to represent a more aggressive, "real-life" type of driving.

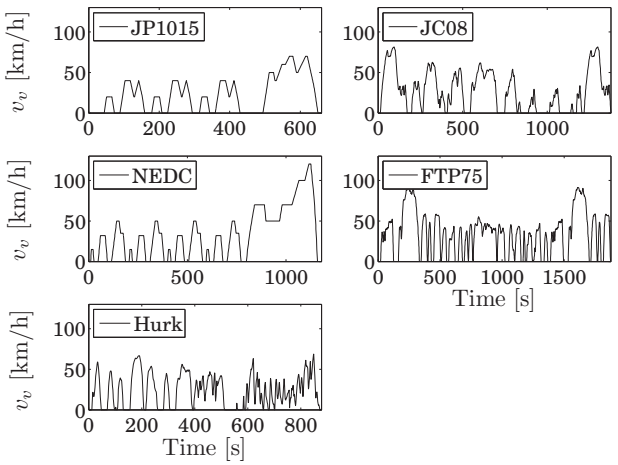

Fig. 3. Five typical driving cycles: Japan 10-15 (JP1015), Japan Cycle 08 (JC08), New European Driving Cycle (NEDC), Federal Test Procedure 75 (FTP75) and a "real-life" driving cycle (Hurk).

A. Problem Reduction

The optimization problem defined by (18), has 2 control variables and 3 state variables. Three methods are proposed to reduce these degrees of freedom, thereby reducing the complexity of this optimization problem.

1) Combining Control Inputs: control input $u_2 = T_{ice}$ is only defined for $u_1 = \{\phi(2), \phi(3)\}$. Hence, for finite control input length M for T_{ice}, the two control inputs may be combined into one:

$$u_1 = \left[\phi(1)\begin{bmatrix}\phi(2)\\ T_{ice}(1)\end{bmatrix}, \begin{bmatrix}\phi(2)\\ \cdots\end{bmatrix}, \ldots, \begin{bmatrix}\phi(2)\\ T_{ice}(M)\end{bmatrix}, \begin{bmatrix}\phi(3)\\ T_{ice}(1)\end{bmatrix}, \begin{bmatrix}\phi(3)\\ \cdots\end{bmatrix}, \begin{bmatrix}\phi(3)\\ T_{ice}(M)\end{bmatrix}\right]^T. \tag{20}$$

2) A Priori Optimization 1: it is assumed that with ICE Driving, the optimal control input u_2 is independent of the optimal control input u_1. Then, the optimal T_{ice} can be calculated for each $\{x, w\}$ a priori

$$T_{ice,k} = \arg\min_{T_{ice,k}} \ \Delta m_f(x_k, u_k, w_k) \mid_{\phi_k=3} . \tag{21}$$

such that control input u_2 may be omitted for $\phi = 3$. Using this optimization, it is observed that the ICE's acceleration is relatively small. With the assumption that the corresponding torque, due to the ICE's inertia, is negligible, state x_1 may be omitted. Note that during driving mode shifts, the acceleration can be estimated without x_1, as current and desired ICE's speed are known during driving mode shifts.

3) A Priori Optimization 2: it is assumed that with FW Charging, the optimal control input u_2 is independent of the optimal control input u_1. Then, the optimal T_{ice} can be calculated for each $\{x, w\}$ a priori, with the *combustion efficiency* $\eta_{ice} = \Delta m_f/(T_{ice}\omega_e)$ as optimization criterion:

$$T_{ice,k} = \arg\min_{T_{ice}} \ \eta_{ice}(x_k, u_k, w_k) \mid_{\phi_k=2} . \tag{22}$$

such that control input u_2 may be omitted for $\phi = 2$. Note that this is severe assumption, as E_f is directly influenced by T_{ice}; by optimizing T_{ice}, without considering the system's energy balance, a sub-optimal solution is found. The main advantage of this reduction, however, is that in combination with (21), the optimization problem of finding the optimal driving mode and generated engine torque, is reduced to finding the optimal driving mode only.

B. Dynamic Programming

Dynamic Programming is applied to solve the optimization problem reduced by (20) and (21) (DP1), and the optimization problem reduced by (21) and (22) (DP2). For comparison reasons, the baseline vehicle without hybrid module (BL) is also simulated using the same model (including the flywheel module mass), with restricted control input $\phi = 3$. The effect of the flywheel module mass (27 kg) on the fuel consumption is expected to be negligible.

V. RESULTS

Fig. 4 shows the simulation results of the DP1 and DP2 optimization problems, for the NEDC. From top to bottom, the five graphs depict, respectively, the vehicle's velocity, the optimal driving modes, the optimal generated engine net-torque (incl. drag losses), the FW's energy content, and the power losses due to the slipping drive clutch and cranking of the ICE. It can be seen that the optimal EMS (i.e., ϕ and T_e) for DP1 and DP2 are very similar. The FW is used as follows: the FW launches the vehicle; the ICE charges the FW during vehicle acceleration at low velocity; the FW propels the vehicle at low constant velocities; the FW is charged by regenerative braking; the ICE propels the vehicle at higher vehicle velocities. Table IV summarizes the fuel

consumption results of the BL, DP1, and DP2 optimization problems, for the considered driving cycles. The fuel saving potential of the hybrid drive train ranges in between 20% and 39%, dependent on the chosen driving cycle. The lower fuel savings with the NEDC and FTP75 may be explained with the highway-parts, where the flywheel is not used. The fuel saving potential with DP2 is slightly less ($\leq 1.0\%$) than with DP1. Obviously, no reduction in fuel saving is desired, but with DP2, the optimization problem of finding the optimal driving mode and generated engine torque, is reduced to finding *only* the optimal driving mode, which greatly reduces the complexity of this problem.

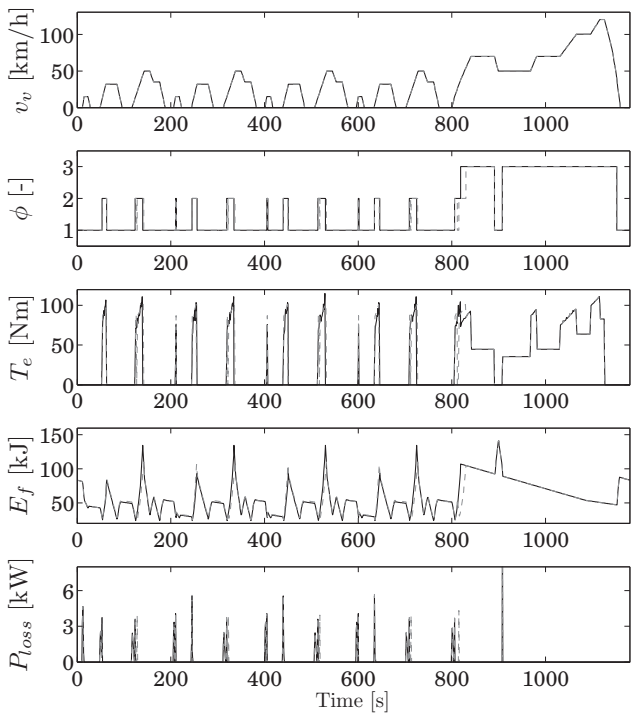

Fig. 4. Optimal EMS of the DP1 (solid gray line) and DP2 (dashed black line) optimization problems, for the NEDC.

TABLE IV
FUEL CONSUMPTION FOR FIVE DRIVING CYCLES

	Fuel consumption (l/100km)		
Driving cycle	BL	DP1	DP2
JP1015	6.06	3.82 (-37.0%)	3.88 (-36.0%)
JC08	5.76	3.87 (-32.8%)	3.89 (-32.5%)
NEDC	5.75	4.60 (-20.0%)	4.63 (-19.5%)
FTP75	5.48	3.99 (-27.2%)	4.02 (-26.6%)
Hurk	7.91	4.78 (-39.6%)	4.82 (-39.1%)

VI. CONCLUSIONS AND FUTURE WORK

A dynamic simulation model is presented of a flywheel-based mechanical-hybrid drive train. An optimization problem is defined, which minimizes the fuel consumption, while respecting the system's dynamics, kinematics, and (comfort-related) constraints. Dynamic programming is used to solve the optimization problem, which is reduced by using three methods; each with a different degree of reduction. Simulation results show that with the presented hybrid drive train, the fuel saving potential ranges between 20 and 39% with respect to its conventional equivalence, dependent on the chosen driving cycle. Moreover, these results show that the optimization problem can be reduced, with minor consequences to the fuel saving ($\leq 1\%$). The optimal controller provides a benchmark for the fuel saving potential, and together with the proposed reductions, it can form a basis for the design of a close-to-optimal, online-implementable controller, which is the subject for future work.

REFERENCES

[1] B. Vroemen, P. Debal, L. Römers, and M. Maessen, "Mechybrid; a low-cost mechanical hybrid," in *Proc. of the 6th Int. Conf. on Continuously Variable and Hybrid Transmissions, Maastricht, Netherlands*, 2010.

[2] K. van Berkel, L. Römers, T. Hofman, B. Vroemen, and M. Steinbuch, "Design of a low-cost hybrid powertrain with large fuel savings," in *Proc. of the 25th Int. Electric Vehicle Symposium, Shenzen, China*, 2010.

[3] K. Mäder, "Continuously variable transmission: Benchmark, status and potentials," in *Proc. of the 4th Int. CTI Symp, Berlin, Germany*, 2005.

[4] L. Guzella and S. Sciarreta, *Vehicle propulsion systems: introduction to modeling and optimization*, 2nd ed. Springer-Verlag, 2007.

[5] B. Bonsen, T. Klaassen, R. Pulles, M. Simons, M. Steinbuch, and P. Veenhuizen, "Performance optimisation of the push-belt cvt by variator slip control," *Int. J. of Vehicle Design*, vol. 39, no. 3, pp. 232–256, 2005.

[6] S. van der Meulen, B. de Jager, F. Veldpaus, and M. Steinbuch, "Combining extremum seeking control and tracking control for high-performance cvt operation," in *Proc. of the 49th IEEE Conf. on Decision and Control, Atlanta, U.S.A.*, 2010.

[7] T. Hofman, "Framework for combined control and design optimization of hybrid vehicle propulsion systems," Ph.D. dissertation, Technische Universiteit Eindhoven, Netherlands, 2007.

[8] M. Koot, J. T. B. A. Kessels, B. de Jager, W. P. M. H. Heemels, P. P. J. van den Bosch, and M. Steinbuch, "Energy management strategies for vehicular electric power systems," *IEEE Transactions on Vehicular Technology*, vol. 54, no. 3, pp. 771–782, 2005.

[9] Y. Zhu, Y. Chen, Z. Wu, and A. Wang, "Optimisation design of an energy management strategy for hybrid vehicles," *Int. J. of Alternative Propulsion*, vol. 1, no. 1, pp. 47–62, 2006.

[10] Y. Huang, "A hybrid power driving system with an energy storage flywheel for vehicles," in *Proc. of the SAE Comm. Veh. Eng. Congress, Rosemont, Illinois, U.S.A.*, 2007.

[11] O. Sundstrom, D. Ambuhl, and L. Guzella, "On implementation of dynamic programming for optimal control problems with final state constraints," *Oil Gas Sci. Technol.*, vol. 65, no. 1, pp. 91–102, 2010.

[12] R. Bellman, *Dynamic Programming*. Princeton University Press, 1962.

[13] F. Salmasi, "Control strategies for hybrid electric vehicles: Evolution, classification, comparison, and future trends," *IEEE Transactions On Vehicular Technology*, vol. 56, no. 5, pp. 2393–2404, 2007.

[14] S. Wright, "Control of ivt-based vehicles by intelligent selection between alternative solutions," Ph.D. dissertation, University of Lancaster, U.K., 2006.

[15] E. Spijker, "Steering and control of a cvt based hybrid passenger car," Ph.D. dissertation, Technische Universiteit Eindhoven, Netherlands, 1994.

[16] D. Kok, "Design optimization of a flywheel hybrid vehicle," Ph.D. dissertation, Technische Universiteit Eindhoven, Netherlands, 1999.

[17] R. Pfiffner, L. Guzzella, and C. H. Onder, "Fuel-optimal control of cvt powertrains," *IFAC Control Engineering Practice*, vol. 11, no. 3, pp. 329 – 336, 2003.

[18] K. van Berkel, T. Hofman, B. Vroemen, and M. Steinbuch, "Optimal regenerative braking with a push-belt cvt: an experimental study," in *Proc. of the 10th Int. Symp. on Advanced Vehicle Control, Loughborough, U.K.*, 2010, pp. 67–72.